HHS Public Access

Author manuscript

Int J Obes (Lond). Author manuscript; available in PMC 2024 December 01.

Published in final edited form as:

Int J Obes (Lond). 2024 June ; 48(6): 841–848. doi:10.1038/s41366-024-01481-y.

Obesity affects brain cortex gene expression in an APOE genotype and sex dependent manner

Harshul Pandit[1], **Nahdia S. Jones**[1], **G. William Rebeck**[1,*]

[1]Department of Neuroscience, Georgetown University Medical Center, 3970 Reservoir Road N.W., Washington D.C. 20007.

Abstract

Objective: Obesity is the top modifiable risk factor for Alzheimer's disease. We hypothesized that high fat diet (HFD)-induced obesity alters brain transcriptomics in APOE-genotype and sex dependent manners. Here, we investigated interactions between HFD, APOE, and sex, using a knock-in mouse model of the human APOE3 and APOE4 alleles.

Methods: Six-month-old APOE3-TR and APOE4-TR mice were treated with either HFD or control chow. After 4 months, total RNA was extracted from the cerebral cortices and analyzed by poly-A enriched RNA sequencing on the Illumina platform.

Results: Female mice demonstrated profound HFD-induced transcriptomic changes while there was little to no effect in males. In females, APOE3 brains demonstrated about five times more HFD-induced transcriptomic changes (399 up-regulated and 107 down-regulated genes) compared to APOE4 brains (30 up-regulated and 60 down-regulated). Unsupervised clustering analysis revealed two gene sets that responded to HFD in APOE3 mice but not in APOE4 mice. Pathway analysis demonstrated that HFD in APOE3 mice affected cortical pathways related to feeding behavior, blood circulation, circadian rhythms, extracellular matrix, and cell adhesion.

Conclusions: Female mice and APOE3 mice have the strongest cortical transcriptomic responses to HFD related to feeding behavior and extracellular matrix remodeling. The relative lack of response of the APOE4 brain to stress associated with obesity may leave it more susceptible to additional stresses that occur with aging and in AD.

Keywords

APOE; RNA sequencing; obesity; cerebral cortex; APOE-TR

[*]To whom correspondence should be addressed: G. William Rebeck, Ph.D., Professor, Department of Neuroscience, Georgetown University Medical Center, New Research Building, Room WP-15, 3970 Reservoir Road, N.W., Washington D.C. 20007; gwr2@georgetown.edu.

AUTHOR CONTRIBUTIONS: HP and GWR wrote the manuscript. HP was responsible for cortical tissue processing, RNA extractions for RNA-sequencing, and bioinformatics analysis. NJ and GWR designed and executed animal experiments. HP and GWR analyzed the data, identified outliers, and interpreted the results. GWR mentored HP and NJ, and supported this study. All authors read and approved the final manuscript.

DISCLOSURE (CONFLICT OF INTERESTS)

The authors declare that they have no conflict of interest with the contents of this article.

INTRODUCTION

Alzheimer's disease (AD) is a progressive neurodegenerative disease that is associated clinically with cognitive decline and neuropathologically with an early appearance of amyloid plaques across brain regions and a later region-specific spreading of phospho-tau neurofibrillary tangles (1). The amyloid plaques first appear in the cerebral cortex (2), with tangles appearing early in the entorhinal cortex and hippocampus (3). The strongest genetic risk factor for AD is *APOE4* (4), which is associated with an earlier age of AD onset (seven years per *APOE4* allele (5)) and higher levels of amyloid (6, 7). APOE4 provides an earlier risk of AD in women than in men [5]. The importance of the APOE4 genotype in AD is reflected in its routine use in clinical studies of environmental risk factors, disease progression, and response to experimental therapies (8).

Midlife obesity is the most prominent modifiable risk factor for AD (9, 10). Midlife obesity increases the risk of AD over two fold (8). There is a high prevalence of obesity in the US, with about 40% of adults affected (11, 12), increasing the predicted number of AD cases in the coming years (13). Given this association, several anti-obesity and anti-diabetes drugs are being evaluated for efficacy against AD (14).

These strong effects of both APOE genotype and obesity on the risk of AD have led to several mouse model studies on gene-environment interactions. These studies have utilized APOE targeted replacement mice (APOE-TR), in which the mouse APOE coding sequence was replaced by human APOE sequences (15). On several types of high-fat diets (HFDs), APOE3 mice tended to gain more weight than APOE4 mice (16–20) (although exceptions exist (21, 22)), and weight gain correlated with measures of glucose intolerance and visceral adipose tissue. Treatments with HFDs revealed effects on gliosis (23), neuroinflammation (24), and behavior (25).

Several previous studies with HFD in mouse models have characterized brain gene expression using transcriptomics strategies. In young wild-type mice, HFD altered transcripts related to neurogenesis, synapses, and calcium signaling in the cortex (26). In an AD mouse model, HFD increased amyloid plaques and induced immune response networks in APOE4 (27) and wild-type backgrounds (28). A mouse model with impaired lipid metabolism showed HFD induced changes to transcripts related to neurogenesis, synaptic plasticity, long-term and potentiation (29). Our current study takes a comprehensive transcriptomic approach to characterize HFD, APOE, and sex interactions in a single study.

We used the APOE-TR mouse model to analyze the cerebral cortex transcriptome through RNA-sequencing to define how HFD alters gene expression in APOE genotype- and sex-influenced ways. We found greater transcriptome changes in response to obesity in APOE3 mice compared to APOE4 mice, and in female mice compared to male mice. The identified transcripts provide a gene expression profile for mechanistic insight into the complex responses of the cerebral cortex to obesity.

METHODS

Animals

All animal experiments, procedures, and handling were performed according to protocols approved by the Georgetown University Institutional Animal Care and Use Committee (IACUC). The IACUC strictly follow all ethical standards and guidelines for animal welfare, including the National Institutes of Health Guide for the Care and Use of Laboratory Animals.

We used C57BL/6J APOE-TR mice, a knock-in model that replaced the mouse *Apoe* gene with individual human APOE alleles (15). The mice are thus a model with normal APOE expression (30), and have been used in several studies of the combined physiological effects of APOE and obesity (16–22). The mice are maintained as APOE3 or APOE4 homozygotes. Six-month old, male and female, APOE3-TR and APOE4-TR mice (n=7–8, per group, randomly assigned) were fed either a HFD containing 45% kcal fat (D12451, Research Diets, New Brunswick, NJ, USA) or a matching control diet with 10% kcal fat (control chow, D12450H, Research Diets, New Brunswick, NJ, USA). The HFD used here closely resembled Western diets, featuring a high-fructose component. To mimic early obesity changes, we treated mice for 16 weeks, with free access to water and chow throughout the study. Sample size estimation, and the metabolic and behavior effects of obesity on these mice are described in our previous studies (22, 23).

Tissue collection

Mice were euthanized by CO_2 and intracardially perfused with 0.1M phosphate-buffered saline solution (PBS, pH 7.4) prior to brain collection. This perfusion step efficiently removes peripheral blood from the brain vasculature. One hemibrain from each mouse was dissected into the cerebral cortex, hippocampus, and cerebellum and snap frozen. Four samples from each group of mouse brains were used in the subsequent analyses.

RNA isolation

We isolated cerebral cortex from the mice for analysis because it is the earliest location of Aβ deposition in humans (2) and is affected in an amyloid model on this APOE-TR background (31). A total of 30–40 mg frozen cerebral cortex from each mouse was homogenized in 600 μL of Trizol reagent (Invitrogen, Waltham, MA, USA) using a glass tissue homogenizer. Trizol homogenates were phase-separated using chloroform, followed by a column-based extraction kit as per manufacturer instructions (Invitrogen). Briefly, after adding chloroform to Trizol homogenate, the upper clear phase was transferred to the column to capture precipitated RNA. After centrifugation and washing steps to remove Trizol carry-over chemicals, on-column DNase digestion was performed. After column wash steps, purified RNA was eluted in 50 μL nuclease-free water for RNA-sequencing. RNA concentration was measured using a nanodrop spectrophotometer (Thermofisher Scientific, Waltham, MA, USA) and RNA integrity analysis was performed on a bioanalyzer (TapeStation 2100, Agilent Technologies, Santa Clara, CA, USA). RNA extracted from all samples demonstrated an RNA Integrity Number (RIN) greater than 8.0, and was processed for library preparation. Samples were blinded and further sample quality control

(QC), library preparations, and sequencing reactions were conducted at GeneWiz (South Plainfield, NJ, USA), to ensure unbiased data acquisition.

Library preparation and next generation RNA sequencing

At Genewiz, RNA samples were quantified using A Qubit 2.0 Fluorometer (ThermoFisher Scientific), and the sequencing libraries were prepared using the NEBNext Ultra II RNA Library Prep Kit for Illumina (New England Biolabs, Ipswich, MA, USA). Briefly, mRNAs were initially enriched with Oligo d(T) beads and fragmented for 15 minutes at 94 °C. First strand and second strand cDNA were synthesized, end repaired, and adenylated at 3'ends. Universal adapters were ligated to cDNA fragments, followed by index addition and library enrichment by PCR with limited cycles. The sequencing libraries were validated on the TapeStation (Agilent Technologies), and quantified by using THE Qubit 2.0 Fluorometer as well as by quantitative PCR (KAPA Biosystems/Roche, Basel, Switzerland).

The sequencing libraries were multiplexed and clustered onto a flow cell. The highest read-depth we could achieve per flow-cell was ~400 million (technical limitation). It's widely accepted in the field that achieving at least 20 million read depths is optimal for capturing the entire transcriptome. To maintain balanced quality and minimize experimental variables, we opted for a sample size (n) of 16 per flow cell. To reduce intra-experimental and intra-day variables, all four groups for each sex were run on the same flow cell. Specifically, flow cell-1 (female) had n=4 per group, totaling n=16, while flow cell-2 (male) had n=3–4 per group, totaling n=15. After clustering, the flowcell was loaded onto the Illumina HiSeq instrument. The samples were sequenced using a 2×150bp Paired End configuration. Image analysis and base calling were conducted by the HiSeq Control Software. Raw sequence data generated from Illumina HiSeq was converted into fastq files and de-multiplexed using Illumina bcl2fastq 2.20 software. One mismatch was allowed for index sequence identification.

RNA-seq analysis

All sequencing libraries were processed identically and analyses were carried out using R v.4.0.2 suite. After confirmation of the quality of the raw data, sequence reads were trimmed to remove possible adapter sequences and nucleotides with poor quality using Trimmomatic v.0.36. The trimmed reads were mapped to the Mus musculus reference genome GRCm38 using the STAR aligner v.2.5.2b to generate BAM files. Unique gene hit counts were calculated by using featureCounts (Subread v.1.4.6). To identify differentially expressed genes, we used R/Bioconductor DESeq2 v.1.16.1. A Principal Component Analysis (PCA) was performed using the "plotPCA" function within the DESeq2 R package. Group comparisons were performed using FDR cut-off=0.05 and fold-change=1.5. Genes with adjusted P values < 0.05 were identified as differentially expressed genes (DEGs) in HFD compared to control.

Downstream analysis

We first filtered out the low expressed genes by establishing threshold of 0.5 counts per million (CPM) in at least three samples. Filtered data were then transformed using EdgeR and analyzed for PCA. We conducted a data-driven, unbiased quality control

(QC) approach before proceeding with the downstream processing of RNA-seq data. This QC method involved unsupervised clustering followed by PCA analysis, which revealed biological replicates not clustering within their respective experimental groups. This divergence was attributed to exceeding the cumulative threshold of variation, likely due to potential contamination during library preparation, the presence of inhibitors, suboptimal coverage, variations in animal treatment, or tissue collection procedures. Subsequently, after identifying outliers using this data-driven statistical method, we retained only the top three samples from each group, which formed cohesive clusters. We then performed hierarchical gene clustering by employing unsupervised k-means approach using R/Bioconductor MultiClust v.3.16. MA plots and Heat plots were derived output from R suite using processed data for each comparison. We further analyzed each cluster of genes identified for biological pathway enrichment using gene ontology analysis (GO:BP), and modeled the pathways using a 0.3 cut-off. To avoid the overwhelming sex effects on cerebral cortex gene expression, we conducted all subsequent analyses separately for male and female groups.

RESULTS

Study modeling and animal characteristics

To investigate how obesity interacts with APOE genotype and sex, we had previously treated 6-month-old APOE-TR mice with either HFD (45% fat) or a matching control diet (10% fat) for 4 months (Figure 1A) (22). The HFD treatment induced weight gain, metabolic responses, and neuroinflammation in APOE- and sex-dependent manners (22, 23). To now explore the effects of HFD on gene expression in the cerebral cortex, we selected four mice from each of the eight subgroups (HFD/control, APOE3/APOE4, male/female). We focused on the cerebral cortex, where Aβ accumulation first appears, 10–20 years before clinical symptoms of AD (32). This analysis consisted of 31 mice in total (one sample was lost in the processing). Mice were chosen to represent the scale of weight gain that had previously been observed (Figure 1B).

RNA sequencing, PCA analysis, and QC exclusion

Dissected cerebral cortices were collected after euthanasia and were used to isolate ultra-pure RNA (RIN>8). We used poly-A enriched RNA for sequencing on the Illumina platform (Figure 2A). We achieved a total of ~854 million paired-end reads, with about 27 million reads per sample and an average unique fragment mappability of ~93%.

We performed unbiased QC prior to downstream processing of RNA-seq data. We filtered out the low-expressed genes and then performed an initial PCA and hierarchical clustering. Nearly all RNA-seq datasets separated into distinct clusters based on the eight different groups. However, this QC approach identified individual samples which did not cluster well within their group. These samples were generally the mice with either lowest weight gain in HFD groups or highest weight gain in control groups (five of the seven samples excluded) (Figure 1B). These data suggest that the absolute level of weight gain is an important factor in the magnitude of transcriptional effects in the brain. We focused subsequent analyses only on the top three clustered samples within each group (Supplementary Figure S1).

Filtered data were then transformed using EdgeR, and PCA was performed. As expected, male and female sex were strongly separated regardless of other variables in the PCA (Figure 2B). To avoid the overwhelming sex effects on cerebral cortex gene expression, we conducted all subsequent analyses separately for male and female groups (Figures 2C and 2D). In females, PCA showed a strong separation of APOE3 and APOE4 groups overall (Figure 2C, upper panel). When these groups were then separated by diet (Figure 2C, lower panel), females also showed a clear separation of the four subgroups (E3 control, E3 HFD, E4 control, E4 HFD). In contrast, male mice failed to exhibit similar separation of APOE clusters (Figure 2D), either without (upper panel) or with (lower panel) consideration of the type of diet. Thus, APOE genotype and HFD had more consistent effects on cerebral cortex transcriptomics in female mice than in male mice.

HFD has profound impact on the cerebral cortex transcriptome

We investigated these mRNA profiles in order to identify the differentially expressed genes (DEG) by APOE genotype and diet within each sex (complete lists in Supplementary Tables S1 and S2). APOE3 female brains demonstrated 506 significant DEGs in response to HFD: 399 up-regulated and 107 down-regulated (Figure 3A, upper left panel). APOE4 female brains demonstrated only 90 DEG in response to HFD: 30 up-regulated and 60 down-regulated (Figure 3A, lower left panel). These up and down-regulated genes showed similar expression patterns across samples (Control and HFD) (Figure 3A, right panels). In contrast, male brains demonstrated very few significant DEGs overall. In APOE3 brains, there were only 6 significant DEGs in response to HFD: 5 up-regulated, and 1 down-regulated (Figure 3B, upper panel). In APOE4 male brains, there was only 1 significant DEG, which was down-regulated (Figure 3B, lower panel). Thus, in female mouse brains, APOE3 HFD induces significant expression changes in five-fold more genes compared to APOE4. In male brains, by contrast, HFD had little to no effect on gene expression in both APOE3 and APOE4 environments. Due to this overwhelming sex difference, our subsequent analyses could only be conducted on female mice.

Clustering analysis demonstrated compromised APOE4 microenvironment

In order to identify the patterns of the effects of HFD on gene expression in female APOE3 mouse brains compared to APOE4 mouse brains, we ran a larger, unsupervised clustering analysis of the top 2000 genes with the highest standard deviations. Using unbiased K-means clustering of the groups (E3 Control, E3 HFD, E4 Control, E4 HFD), we identified four separate clusters of genes, denoted A-D (Figure 4A; Supplementary Table S3). These four gene clusters were analyzed for pathways that were enriched. Cluster B and cluster D demonstrated distinct patterns of gene expression. In cluster B, genes that were up-regulated after HFD in APOE3 brains were already elevated in the control APOE4 brains and were not altered by HFD (Figure 4A). These genes were enriched in pathways related to feeding behavior, regulation of blood circulation, and circadian rhythms. This cluster also contained a group of connected pathways related to adenylate cyclase signaling. 50% of cluster B genes are not yet characterized (Supplementary Table S3), suggesting that more detailed pathways will be defined in the future. When expanding the subset analysis to include both female and male mice together (see Supplementary Figure S2), it became evident that male

mice failed to respond to HFD in both APOE3 and APOE4. In addition, APOE4 male mice had lower levels of these cluster B genes than APOE4 female mice.

Cluster D genes showed a different pattern than the genes in cluster B. Cluster D genes, comprising 50% of the genes in the overall cluster analysis, exhibited similar levels of expression between the APOE3 and APOE4 groups under control conditions. However, APOE3 brains showed an up-regulation of these genes after HFD, while APOE4 brains had little change to their low expression after HFD. Cluster D enriched pathways were related to extracellular matrix, cell adhesion, and tissue/organ development.

Differentially expressed genes related to APOE genotype

These previous analyses focused on the effects of HFD on gene expression. However, our experimental design allowed the analysis of the effects of APOE genotype, in the absence or in the presence of HFD. We conducted a comparison of APOE genotype-related differentially expressed genes (DEGs, FDR=0.1, FC ≥ 1.5) in both control and HFD groups, stratified by sex (see Supplementary Table S4). Notably, female brains exhibited a substantially higher number of APOE genotype-related DEGs under control conditions (268 compared to 29 in males) and after HFD exposure (252 compared to 45 in males) (Supplementary Table S4, first and second tabs). However, when samples from both sexes were combined for analysis, only 51 DEGs were observed under control conditions, and 36 DEGs were identified after HFD exposure (Supplementary Table S4, third and fourth tabs).

Figure 5 shows the 51 DEGs that were present under control diet conditions (left circle) and 36 DEGs that were present under HFD conditions (right circle). We compared these two datasets, and found that 26 of these DEGs were shared between control and HFD environments (Figure 5, overlapping area). We compared the 51 DEGs from APOE mice on control diets (Figure 5, lower lists) with a public database from a study that included comparisons at three different ages (3, 12, and 24 months) (33). Of the 51 DEGs identified in our study, 39 had previously been identified in this database (some of our additional DEGs may be due to recent expansions of the annotations in the mouse genome). Among these 39 genes, 72% exhibited significant differences in the same direction in both databases, while another 13% of DEGs here showed trends that were not statistically significant in the published database. The strongest agreements across ages were seen *for Serpina3, Oscar, Wdfy1, Fank1, Eps8I1*, and *Anax4*. We also identified 10 APOE DEGs that were only observed in mice on the HFD (Figure 5, lower right list); only two of these showed significant differences in the previous study (33). Thus, our analysis largely agrees with published work and identifies other APOE-related DEGs that emerge only in the presence of obesity. Complete lists of these genes are provided in Supplementary Table S5.

DISCUSSION

Obesity is a strong environmental risk factor for neurodegeneration (34), with a growing number of individuals categorized as obese each year. In this study, we studied the effects of obesity on brain gene expression, and incorporated sex and APOE genetic variability. We found that HFD had strong effects on transcripts in the cerebral cortex in female mice and in APOE3 mice, but with much smaller effects in male mice and in APOE4 mice.

Increases in gene expression were three to five times more common after HFD compared to decreases. The transcriptomic effects clustered in two distinct patterns: genes that were similarly expressed in control APOE3 and APOE4 mouse brains, but only induced by HFD in the APOE3 brains; and genes that were induced in the APOE3 brains by HFD, but constitutively elevated in the APOE4 brains.

We identified DEGs across sex, APOE genotype, and diet, and defined co-regulated groups of genes by unsupervised K-means clustering. We first found that outliers from the group clustering were from mice that showed the least effect of HFD, as determined by the amounts of weight gain. This observation supports the validity of this approach to studying how diet affects the brain, and emphasizes that the response of the brain to HFD interacts closely with the response of the rest of the body.

Subsequent clustering analysis showed some distinct patterns of gene regulation. Cluster B genes define a model in which genes in APOE3 mouse brains are increased by HFD, but these genes in APOE4 mice are elevated even at control conditions and not increased more by the HFD. Our analysis identified an effect of HFD (in APOE3 mice) on genes related to feeding behavior. Connections between obesity and feeding behavior have generally been noted in gene expression in the hypothalamus (35), which can directly detect plasma metabolic processes as a circumventricular organ (36). We focused on cortical effects, because of its involvement in the earliest processes of neuropathological changes in AD (37). Our studies show cortical changes in gene expression are less extensive than hypothalamic changes, but that feeding behavior is affected broadly in the brain.

The differentially expressed genes (DEGs) in cluster B also included genes affecting blood flow and circadian rhythms. In terms of the regulation of blood flow, there were 22 DEGs in APOE3 mice after HFD, compared to only five in APOE4 mice after HFD. Two genes were significantly increased in APOE3 brains and significantly decreased in APOE4 brains: *Tac1* (Substance P receptor) and *Isl1* (a LIM homeodomain transcription factor). In terms of circadian rhythms, there were 11 DEGs for APOE3 mice after HFD (*Npy2r, Ptgds, Dpyd, Ntrk1, Ngr, Ankfn1, Prkg2, Cartpt, Tyms, Hs3ht2, Kcnh7)*. The only DEG in APOE4 mice after HFD was *Ntrk1*, which increased in APOE3 mice but decreased in APOE4 mice. *Ntrk1* encodes the high affinity receptor for Nerve Growth Factor (NGF), a neurotrophin important in neurodevelopment and neuro-recovery (38). Deficient regulation of circadian rhythm pathways could be related to the sleep problems that precede several types of neurodegeneration (39).

The second pattern of co-regulated genes, Cluster D, also defined genes that were unregulated in APOE4 brains, but which were equivalent to the levels seen in control APOE3 brains. This cluster identified pathways related to extracellular matrix (ECM), cell adhesion, and developmental processes. In terms of the ECM, we found several collagen genes up-regulated in APOE3 but not APOE4 brains by HFD (*Col1a1, Col18a1, Col16a1, Col1a2, Col11a1, Col23a1,* and *Col5a2*). We also found upregulation in ECM proteases (*Adamt39, Adamts6*, and *Adam12*), indicating increased ECM plasticity. Disruption of the ECM is induced by activated astrocytes and microglia, which, in turn, allows easier glial movement and morphological changes (40, 41).

After HFD, there is a greater induction of markers of cellular inflammation (astrocytes and microglia) in APOE3 compared to APOE4 mouse hippocampi (23), supporting the model from the present study that APOE3 brains have responses to obesity-related stress lacking in APOE4 brains. Obesity is associated with peripheral inflammation (42–44) and brain inflammation in the hippocampus (23, 45, 46), and the hypothalamus (47, 48). Neuroinflammation is a contributing factor to the increased risk of AD, particularly in the context of APOE genotype (49), based on genetic analysis (50), animal models (30, 51), and neuropathological findings (52). Obesity, APOE4, and female sex are all strong risk factors for AD. The systems identified here that were affected by HFD (blood flow, circadian rhythms, ECM) support the research driving AD clinical trials on processes of circadian rhythms, vascular factors, and inflammation (53).

In terms of limitations, studies of the effects of HFD are subject to levels of feeding and physical activity that could be related to housing conditions, which introduce variability into the datasets. The present work focuses on a single type of HFD; precise diet composition and length of treatment may account for some of the differences to weight gain and metabolic dysfunctions observed across similar studies of APOE mice (16–22). A more comprehensive study of different HFDs would be informative, as well as larger mouse numbers to identify reproducible brain pathways in brain regions beyond the cerebral cortex analyzed here. Finally, many of the genes differentially expressed after HFD have not been characterized, and thus many biological pathways could be altered that have not been defined.

In conclusion, APOE genotype affected the response of the brain cortex transcriptome to HFD. These effects were most prominent in the brains of female mice, and generally demonstrated patterns of gene up-regulation to obesity in APOE3 mice but not APOE4 mice. These potentially protective mechanisms should promote further research into delaying AD pathogenesis in preclinical models of amyloid and neurofibrillary tangles. They also support the clinical research driving several ongoing clinical trials.

Supplementary Material

Refer to Web version on PubMed Central for supplementary material.

ACKNOWLEDGEMENT:

This work is supported by NIH grants R21 AG074139, R01 AG067258 and R01 NS100704. Authors also would like to acknowledge the Georgetown University Medical Center for providing continuous research support and infrastructure.

DATA AVAILABILITY STATEMENT

The data that support the findings of this study are available from the corresponding author upon reasonable request. All next-generation sequencing raw data for RNA-seq experiments are available from NCBI-SRA, BioProject accession # PRJNA1033375.

REFERENCES

1. Association As. 2022 Alzheimer's disease facts and figures. Alzheimers Dement. 2022;18(4):700–89. [PubMed: 35289055]
2. Braak H, Del Tredici K. The preclinical phase of the pathological process underlying sporadic Alzheimer's disease. Brain. 2015;138(Pt 10):2814–33. [PubMed: 26283673]
3. Hyman BT, Van Hoesen GW, Damasio AR, Barnes CL. Alzheimer's disease: cell-specific pathology isolates the hippocampal formation. Science. 1984;225(4667):1168–70. [PubMed: 6474172]
4. Farrer LA, Cupples LA, Haines JL, Hyman B, Kukull WA, Mayeux R, et al. Effects of age, sex, and ethnicity on the association between apolipoprotein E genotype and Alzheimer disease. A meta-analysis. APOE and Alzheimer Disease Meta Analysis Consortium. JAMA. 1997;278(16):1349–56. [PubMed: 9343467]
5. Reiman EM, Arboleda-Velasquez JF, Quiroz YT, Huentelman MJ, Beach TG, Caselli RJ, et al. Exceptionally low likelihood of Alzheimer's dementia in APOE2 homozygotes from a 5,000-person neuropathological study. Nat Commun. 2020;11(1):667. [PubMed: 32015339]
6. Jansen WJ, Ossenkoppele R, Knol DL, Tijms BM, Scheltens P, Verhey FR, et al. Prevalence of cerebral amyloid pathology in persons without dementia: a meta-analysis. JAMA. 2015;313(19):1924–38. [PubMed: 25988462]
7. Jansen WJ, Ossenkoppele R, Visser PJ. Amyloid Pathology, Cognitive Impairment, and Alzheimer Disease Risk--Reply. JAMA. 2015;314(11):1177–8.
8. Kivipelto M, Ngandu T, Fratiglioni L, Viitanen M, Kareholt I, Winblad B, et al. Obesity and vascular risk factors at midlife and the risk of dementia and Alzheimer disease. Arch Neurol. 2005;62(10):1556–60. [PubMed: 16216938]
9. Nianogo RA, Rosenwohl-Mack A, Yaffe K, Carrasco A, Hoffmann CM, Barnes DE. Risk Factors Associated With Alzheimer Disease and Related Dementias by Sex and Race and Ethnicity in the US. JAMA Neurology. 2022;79(6):584–91. [PubMed: 35532912]
10. Whitmer RA, Gustafson DR, Barrett-Connor E, Haan MN, Gunderson EP, Yaffe K. Central obesity and increased risk of dementia more than three decades later. Neurology. 2008;71(14):1057–64. [PubMed: 18367704]
11. Finkelstein EA, Khavjou OA, Thompson H, Trogdon JG, Pan L, Sherry B, et al. Obesity and severe obesity forecasts through 2030. Am J Prev Med. 2012;42(6):563–70. [PubMed: 22608371]
12. Hales CM, Fryar CD, Carroll MD, Freedman DS, Ogden CL. Trends in Obesity and Severe Obesity Prevalence in US Youth and Adults by Sex and Age, 2007–2008 to 2015–2016. JAMA. 2018;319(16):1723–5. [PubMed: 29570750]
13. Loef M, Walach H. Midlife obesity and dementia: Meta-analysis and adjusted forecast of dementia prevalence in the united states and china. Obesity. 2013;21(1):E51–E5. [PubMed: 23401370]
14. Alford S, Patel D, Perakakis N, Mantzoros CS. Obesity as a risk factor for Alzheimer's disease: weighing the evidence. Obesity Reviews. 2018;19(2):269–80. [PubMed: 29024348]
15. Sullivan PM, Mezdour H, Aratani Y, Knouff C, Najib J, Reddick RL, et al. Targeted replacement of the mouse apolipoprotein E gene with the common human APOE3 allele enhances diet-induced hypercholesterolemia and atherosclerosis. J Biol Chem. 1997;272(29):17972–80. [PubMed: 9218423]
16. Arbones-Mainar JM, Johnson LA, Altenburg MK, Maeda N. Differential modulation of diet-induced obesity and adipocyte functionality by human apolipoprotein E3 and E4 in mice. Int J Obes (Lond). 2008;32(10):1595–605. [PubMed: 18725890]
17. Arbones-Mainar JM, Johnson LA, Torres-Perez E, Garcia AE, Perez-Diaz S, Raber J, et al. Metabolic shifts toward fatty-acid usage and increased thermogenesis are associated with impaired adipogenesis in mice expressing human APOE4. Int J Obes (Lond). 2016;40(10):1574–81. [PubMed: 27163745]
18. Huebbe P, Dose J, Schloesser A, Campbell G, Glüer CC, Gupta Y, et al. Apolipoprotein E (APOE) genotype regulates body weight and fatty acid utilization-Studies in gene-targeted replacement mice. Molecular nutrition & food research. 2015;59(2):334–43. [PubMed: 25381750]

19. Johnson LA, Torres ER, Impey S, Stevens JF, Raber J. Apolipoprotein E4 and Insulin Resistance Interact to Impair Cognition and Alter the Epigenome and Metabolome. Sci Rep. 2017;7:43701. [PubMed: 28272510]
20. Johnson LA, Torres ER, Weber Boutros S, Patel E, Akinyeke T, Alkayed NJ, et al. Apolipoprotein E4 mediates insulin resistance-associated cerebrovascular dysfunction and the post-prandial response. J Cereb Blood Flow Metab. 2019;39(5):770–81. [PubMed: 29215310]
21. To AW, Ribe EM, Chuang TT, Schroeder JE, Lovestone S. The epsilon3 and epsilon4 alleles of human APOE differentially affect tau phosphorylation in hyperinsulinemic and pioglitazone treated mice. PLoS One. 2011;6(2):e16991. [PubMed: 21347323]
22. Jones NS, Watson KQ, Rebeck GW. Metabolic Disturbances of a High-Fat Diet Are Dependent on APOE Genotype and Sex. eNeuro. 2019;6(5).
23. Jones NS, Watson KQ, Rebeck GW. High-fat diet increases gliosis and immediate early gene expression in APOE3 mice, but not APOE4 mice. J Neuroinflammation. 2021;18(1):214. [PubMed: 34537055]
24. Janssen CI, Jansen D, Mutsaers MP, Dederen PJ, Geenen B, Mulder MT, et al. The Effect of a High-Fat Diet on Brain Plasticity, Inflammation and Cognition in Female ApoE4-Knockin and ApoE-Knockout Mice. PLoS One. 2016;11(5):e0155307. [PubMed: 27171180]
25. Mattar JM, Majchrzak M, Iannucci J, Bartman S, Robinson JK, Grammas P. Sex Differences in Metabolic Indices and Chronic Neuroinflammation in Response to Prolonged High-Fat Diet in ApoE4 Knock-In Mice. International journal of molecular sciences. 2022;23(7).
26. Yoon G, Cho KA, Song J, Kim YK. Transcriptomic Analysis of High Fat Diet Fed Mouse Brain Cortex. Front Genet. 2019;10:83. [PubMed: 30838024]
27. Nam KN, Wolfe CM, Fitz NF, Letronne F, Castranio EL, Mounier A, et al. Integrated approach reveals diet, APOE genotype and sex affect immune response in APP mice. Biochim Biophys Acta Mol Basis Dis. 2018;1864(1):152–61. [PubMed: 29038051]
28. Nam KN, Mounier A, Wolfe CM, Fitz NF, Carter AY, Castranio EL, et al. Effect of high fat diet on phenotype, brain transcriptome and lipidome in Alzheimer's model mice. Sci Rep. 2017;7(1):4307. [PubMed: 28655926]
29. So SW, Nixon JP, Bernlohr DA, Butterick TA. RNAseq Analysis of FABP4 Knockout Mouse Hippocampal Transcriptome Suggests a Role for WNT/beta-Catenin in Preventing Obesity-Induced Cognitive Impairment. International journal of molecular sciences. 2023;24(4).
30. Balu D, Karstens AJ, Loukenas E, Maldonado Weng J, York JM, Valencia-Olvera AC, et al. The role of APOE in transgenic mouse models of AD. Neurosci Lett. 2019;707:134285. [PubMed: 31150730]
31. Youmans KL, Tai LM, Nwabuisi-Heath E, Jungbauer L, Kanekiyo T, Gan M, et al. APOE4-specific changes in Abeta accumulation in a new transgenic mouse model of Alzheimer disease. J Biol Chem. 2012;287(50):41774–86. [PubMed: 23060451]
32. Betthauser TJ, Bilgel M, Koscik RL, Jedynak BM, An Y, Kellett KA, et al. Multi-method investigation of factors influencing amyloid onset and impairment in three cohorts. Brain. 2022;145(11):4065–79. [PubMed: 35856240]
33. Zhao N, Ren Y, Yamazaki Y, Qiao W, Li F, Felton LM, et al. Alzheimer's Risk Factors Age, APOE Genotype, and Sex Drive Distinct Molecular Pathways. Neuron. 2020;106(5):727–42 e6. [PubMed: 32199103]
34. Flores-Dorantes MT, Diaz-Lopez YE, Gutierrez-Aguilar R. Environment and Gene Association With Obesity and Their Impact on Neurodegenerative and Neurodevelopmental Diseases. Front Neurosci. 2020;14:863. [PubMed: 32982666]
35. Timshel PN, Thompson JJ, Pers TH. Genetic mapping of etiologic brain cell types for obesity. Elife. 2020;9.
36. Kalin S, Heppner FL, Bechmann I, Prinz M, Tschop MH, Yi CX. Hypothalamic innate immune reaction in obesity. Nat Rev Endocrinol. 2015;11(6):339–51. [PubMed: 25824676]
37. Beach TG. A History of Senile Plaques: From Alzheimer to Amyloid Imaging. J Neuropathol Exp Neurol. 2022;81(6):387–413. [PubMed: 35595841]
38. Aloe L, Rocco ML, Balzamino BO, Micera A. Nerve Growth Factor: A Focus on Neuroscience and Therapy. Curr Neuropharmacol. 2015;13(3):294–303. [PubMed: 26411962]

39. Fifel K, Videnovic A. Circadian and Sleep Dysfunctions in Neurodegenerative Disorders-An Update. Front Neurosci. 2020;14:627330. [PubMed: 33536872]
40. Yu F, Wang Y, Stetler AR, Leak RK, Hu X, Chen J. Phagocytic microglia and macrophages in brain injury and repair. CNS Neurosci Ther. 2022;28(9):1279–93. [PubMed: 35751629]
41. Crapser JD, Arreola MA, Tsourmas KI, Green KN. Microglia as hackers of the matrix: sculpting synapses and the extracellular space. Cell Mol Immunol. 2021;18(11):2472–88. [PubMed: 34413489]
42. Xu H, Barnes GT, Yang Q, Tan G, Yang D, Chou CJ, et al. Chronic inflammation in fat plays a crucial role in the development of obesity-related insulin resistance. J Clin Invest. 2003;112(12):1821–30. [PubMed: 14679177]
43. Baumgarner KM, Setti S, Diaz C, Littlefield A, Jones A, Kohman RA. Diet-induced obesity attenuates cytokine production following an immune challenge. Behav Brain Res. 2014;267:33–41. [PubMed: 24657736]
44. Pistell PJ, Morrison CD, Gupta S, Knight AG, Keller JN, Ingram DK, et al. Cognitive impairment following high fat diet consumption is associated with brain inflammation. J Neuroimmunol. 2010;219(1–2):25–32. [PubMed: 20004026]
45. Rivera P, Perez-Martin M, Pavon FJ, Serrano A, Crespillo A, Cifuentes M, et al. Pharmacological administration of the isoflavone daidzein enhances cell proliferation and reduces high fat diet-induced apoptosis and gliosis in the rat hippocampus. PLoS One. 2013;8(5):e64750. [PubMed: 23741384]
46. Wanrooy BJ, Kumar KP, Wen SW, Qin CX, Ritchie RH, Wong CHY. Distinct contributions of hyperglycemia and high-fat feeding in metabolic syndrome-induced neuroinflammation. J Neuroinflammation. 2018;15(1):293. [PubMed: 30348168]
47. Maric T, Woodside B, Luheshi GN. The effects of dietary saturated fat on basal hypothalamic neuroinflammation in rats. Brain Behav Immun. 2014;36:35–45. [PubMed: 24075847]
48. Thaler JP, Yi CX, Schur EA, Guyenet SJ, Hwang BH, Dietrich MO, et al. Obesity is associated with hypothalamic injury in rodents and humans. J Clin Invest. 2012;122(1):153–62. [PubMed: 22201683]
49. Parhizkar S, Holtzman DM. APOE mediated neuroinflammation and neurodegeneration in Alzheimer's disease. Semin Immunol. 2022;59:101594. [PubMed: 35232622]
50. Lambert JC, Ramirez A, Grenier-Boley B, Bellenguez C. Step by step: towards a better understanding of the genetic architecture of Alzheimer's disease. Mol Psychiatry. 2023.
51. Chen X, Firulyova M, Manis M, Herz J, Smirnov I, Aladyeva E, et al. Microglia-mediated T cell infiltration drives neurodegeneration in tauopathy. Nature. 2023;615(7953):668–77. [PubMed: 36890231]
52. Perez-Nievas BG, Stein TD, Tai HC, Dols-Icardo O, Scotton TC, Barroeta-Espar I, et al. Dissecting phenotypic traits linked to human resilience to Alzheimer's pathology. Brain. 2013;136(Pt 8):2510–26. [PubMed: 23824488]
53. Cummings JL, Osse AML, Kinney JW. Alzheimer's Disease: Novel Targets and Investigational Drugs for Disease Modification. Drugs. 2023;83(15):1387–408. [PubMed: 37728864]

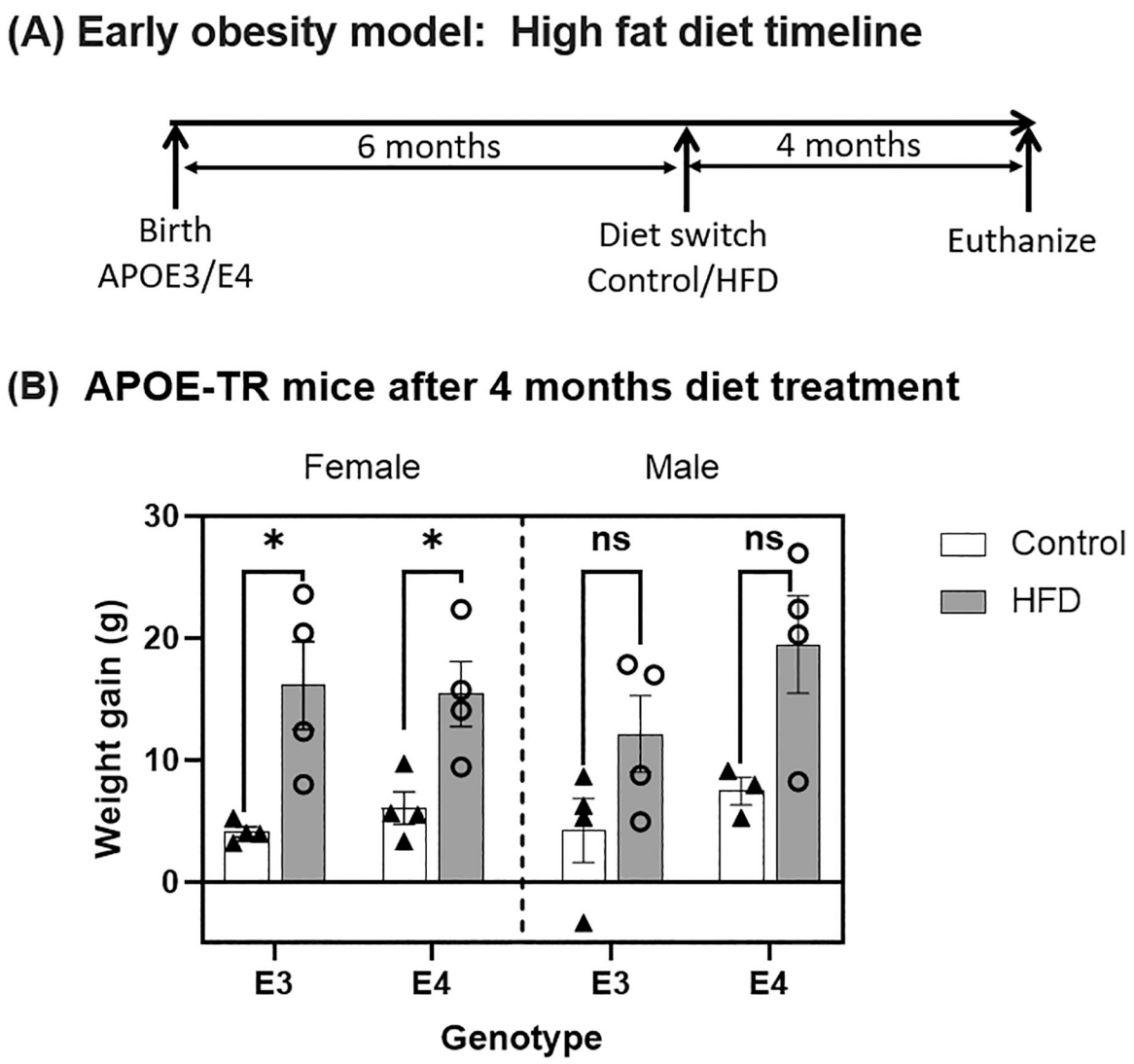

Figure 1. APOE3/4 TR mouse model.

(A) Early obesity model timeline showing APOE-TR mice in both APOE3 and APOE4 groups switched to High Fat Diet (HFD) at 6 months of age. After 4 months of diet treatment, mice were euthanized and brains were collected. **(B)** After 4 months of HFD treatment (n=4 per group), females showed significant weight gain in both APOE3 (p=0.016) and APOE4 (p=0.020) genotypes. In males, APOE4 mice trended toward a significant weight gain (p=0.058) while APOE3 mice showed no significant weight gain (p=0.21). Two-tailed student t-test with equal variance was performed. Control: normal chow diet; HFD: 45% fat with high fructose, p value <0.05 (*) considered significant, na = no significant difference.

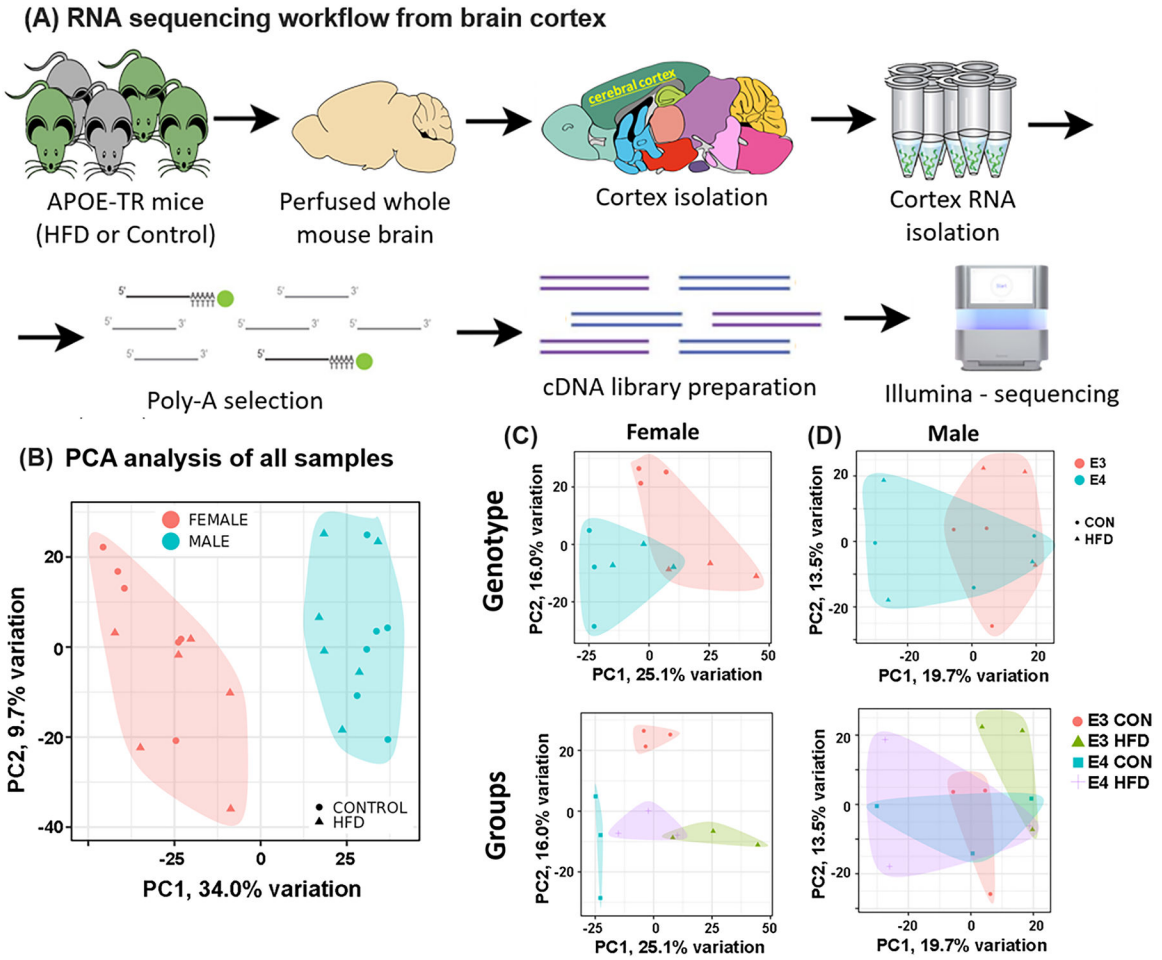

Figure 2. RNA sequencing workflow and PCA analysis.

After euthanasia, brains were first perfused with PBS; cortex, hippocampus, and cerebellum were dissected, and snap-frozen. **(A)** Total cortical RNA was extracted in Trizol, purified using column-based RNA purification, followed by poly-A library preparation, and 150 bp paired sequencing using the Illumina platform. **(B)** After pre-processing and normalization of raw data, principal component analysis (PCA) was performed. PCA analysis showed distinct male (blue) and female (red) clusters. Additional PCA analysis showed females exhibiting distinct clustering of both E3 and E4 groups with or without HFD treatment **(C)**; this distinct clustering was not present in males **(D)**. CON: normal chow diet; HFD: 45% fat with high fructose.

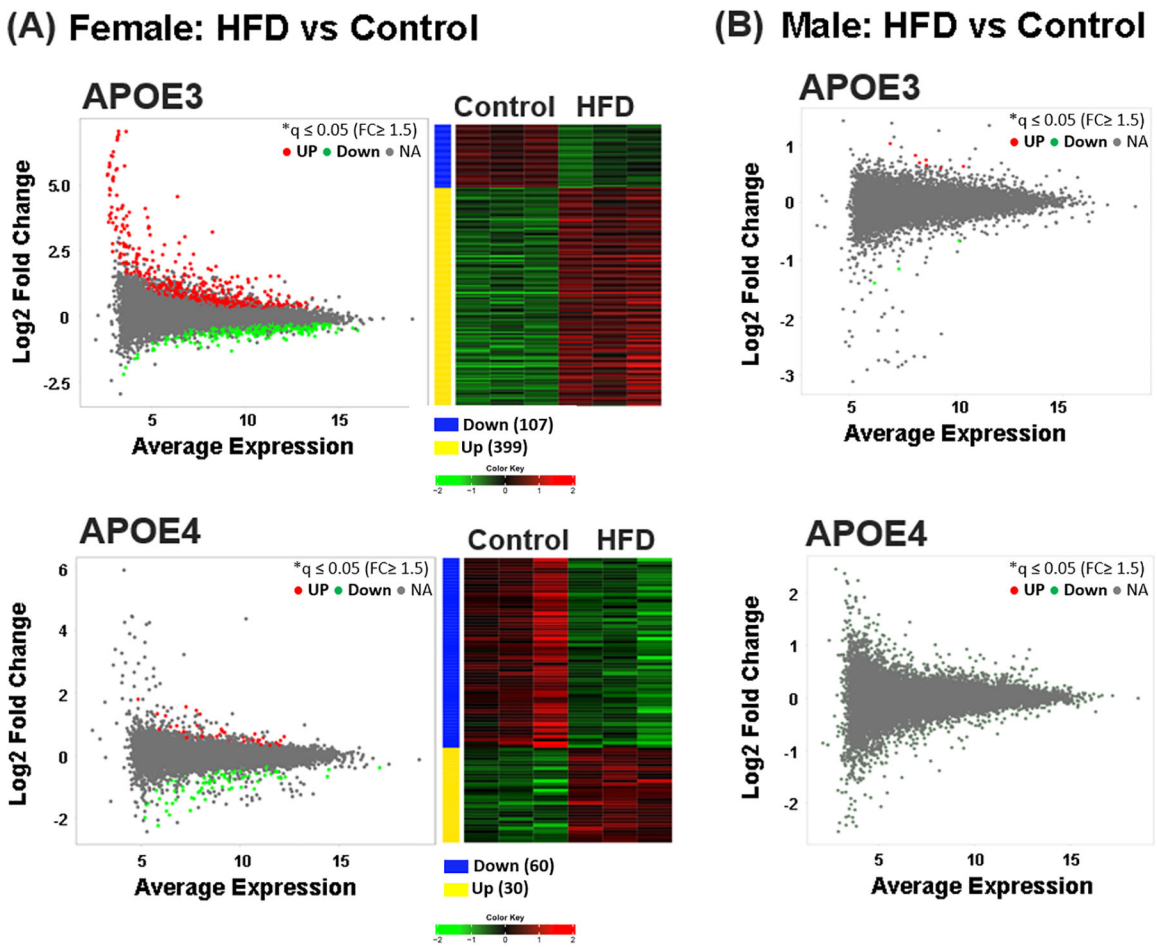

Figure 3. Female sex and APOE3 genotype exhibit more differentially expressed genes (DEGs) in HFD group.

DEseq analysis of the transcriptome of both APOE genotypes in female and male mice. **(A)** MA plots of female group of mice showing significant up-regulated (red) and down-regulated (green) DEGs in APOE3 (506 DEGs, upper panel) and APOE4 (90 DEGs, lower panel). Each MA plot is accompanied with a representative heat map on the right with the numbers of DEGs (blue: down-regulated genes; yellow: up-regulated genes). **(B)** MA Plots of male group of mice showing up-regulated and down-regulated DEGs in APOE3 (6 DEGs) and APOE4 (1 DEG). Cutoff FC=1.5 and FDR=0.05 were applied for the analysis, and DEGs passing an adjusted q-value of <0.05 were considered as significant DEGs. For MA plots and heat maps, up-regulated DEGs are represented in red color and down-regulated genes are represented in green color.

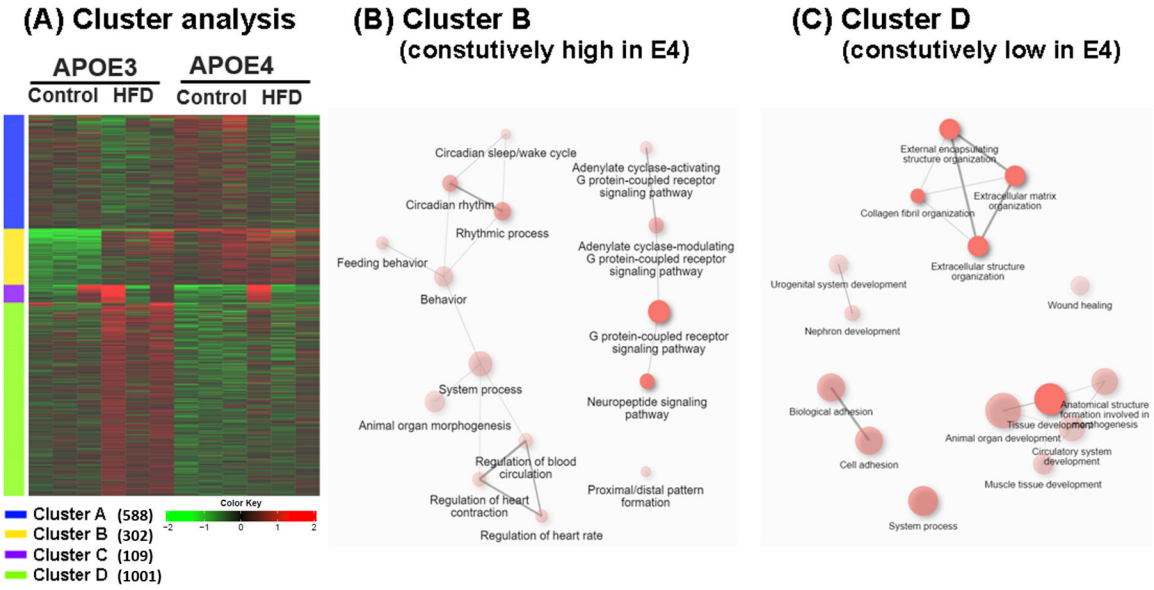

Figure 4. Clustering analysis revealed APOE4 genotype specific impact on transcriptome.

K-mean unsupervised clustering analysis was performed on the top 2000 most variable genes ranked by standard deviation, and grouped into 4 clusters based on expression across experimental groups. **(A)** Heatmap showing 4 clusters, cluster A (588 genes), cluster B (302 genes), cluster C (109 genes), and cluster D (1001 genes). Heatmap expression annotation: Red= increased, Green= decreased. **(B)** The top 15 biological processes (GO:BP) are presented in network annotation for cluster B, which showed those genes which induced in APOE3 upon HFD treatment but are constitutively high in APOE4 genotype. **(C)** Top 15 biological processes (GO:BP) are presented in network annotation for cluster D, which showed those genes which induced in APOE3 upon HFD treatment, but constitutively low in APOE4 genotype (and unresponsive to HFD in APOE4). Biological processes (GO:BP) were ranked based on q-value after FDR = 0.1. Two nodes are connected in network if 30% or more genes are being shared between two biological processes. Red: up-regulated; Green: down-regulated (none).

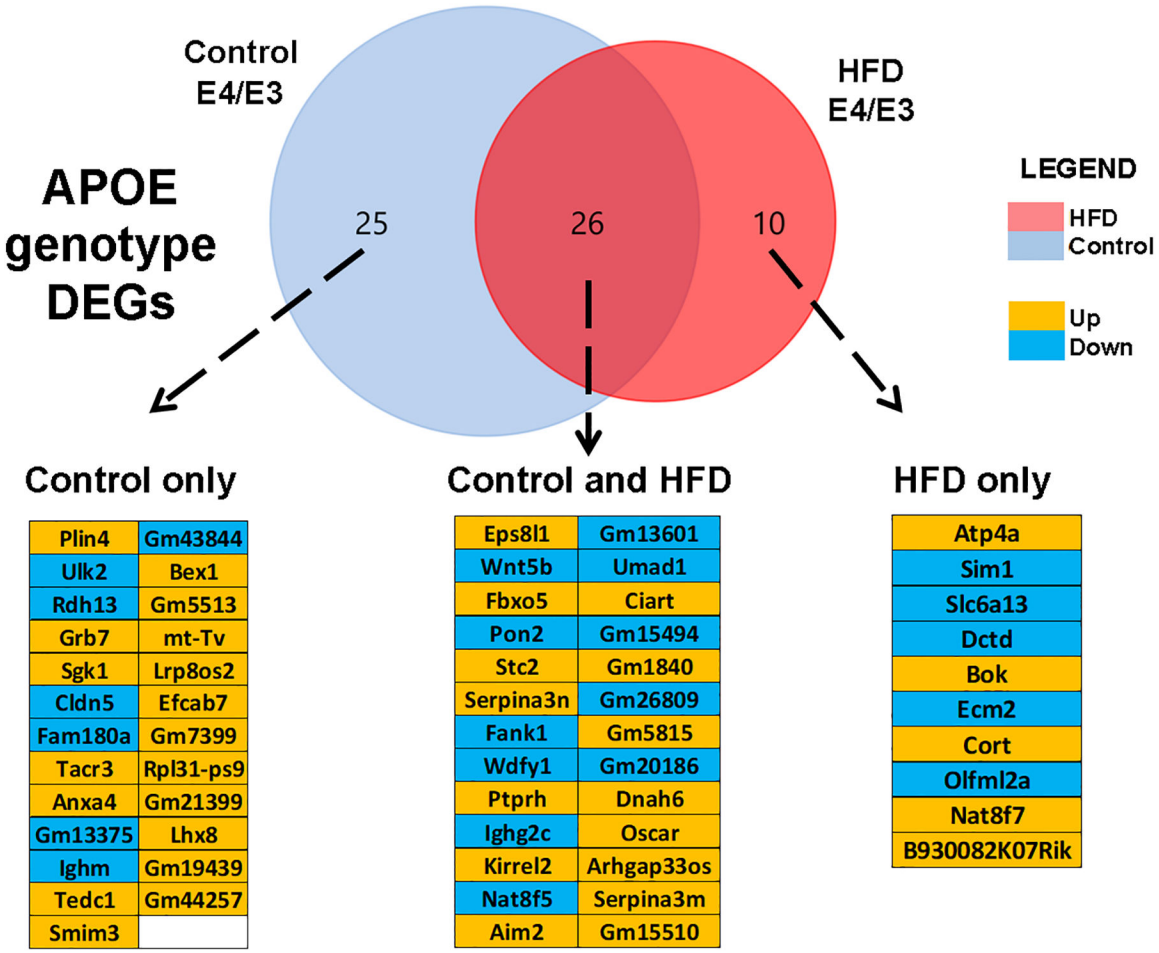

Figure 5. Shared APOE DEGs, including HFD interactions.

APOE differentially expressed genes (DEGs) were identified by comparing APOE4 and APOE3 genotypes including both sexes (male and female). Analysis was performed for control diet (left, blue) and HFD (right, red) separately. We identified 26 constitutive APOE DEGs present in both the control and HFD environments (center). We further identified DEGs which are unaffected by HFD (n=25) and DEGs interacting with HFD only (n=10). In each list, down-regulated APOE4 DEGs (compared to APOE3) are blue, and up-regulated DEGs are in orange. All identified DEGs are considered significant after adjusting FDR to 0.1 with fold change ≥ 1.5.